Biochemical Characterization of Major Bone-Matrix Proteins Using Nanoscale-Size Bone Samples and Proteomics Methodology*[S]

Grażyna E. Sroga‡‖, Lamya Karim‡‖, Wilfredo Colón‡§, and Deepak Vashishth‡‖¶

There is growing evidence supporting the need for a broad scale investigation of the proteins and protein modifications in the organic matrix of bone and the use of these measures to predict fragility fractures. However, limitations in sample availability and high heterogeneity of bone tissue cause unique experimental and/or diagnostic problems. We addressed these by an innovative combination of laser capture microscopy with our newly developed liquid chromatography separation methods, followed by gel electrophoresis and mass spectrometry analysis. Our strategy allows in-depth analysis of very limited amounts of bone material, and thus, can be important to medical sciences, biology, forensic, anthropology, and archaeology. The developed strategy permitted unprecedented biochemical analyses of bone-matrix proteins, including collagen modifications, using nearly nanoscale amounts of exceptionally homogenous bone tissue. Dissection of fully mineralized bone-tissue at such degree of homogeneity has not been achieved before. Application of our strategy established that: (1) collagen in older interstitial bone contains higher levels of an advanced glycation end product pentosidine then younger osteonal tissue, an observation contrary to the published data; (2) the levels of two enzymatic crosslinks (pyridinoline and deoxypiridinoline) were higher in osteonal than interstitial tissue and agreed with data reported by others; (3) younger osteonal bone has higher amount of osteopontin and osteocalcin then older interstitial bone and this has not been shown before. Taken together, these data show that the level of fluorescent crosslinks in collagen and the amount of two major noncollagenous bone matrix proteins differ at the level of osteonal and interstitial tissue. We propose that this may have important implications for bone remodeling processes and bone microdamage formation. ***Molecular & Cellular Proteomics 10: 10.1074/mcp.M110.006718, 1–12, 2011.***

From the Center for Biotechnology and Interdisciplinary Studies‡ Department of Biomedical Engineering‖; and Department of Chemistry and Biological Chemistry§, Rensselaer Polytechnic Institute, Troy, NY 12180

Received November 24, 2010, and in revised form, May 16, 2011
Published, MCP Papers in Press, May 23, 2011, DOI 10.1074/mcp.M110.006718

Bone differs from all other tissues in a body by being composed largely of a mineral (70–90%) and a small amount of total organic material (10–30%) that contains a uniquely large proportion of collagen (approx. 90%). On the basis of this unusual composition, it is generally agreed that collagen plays a critical role in the structure and function of bone tissue. Nonfibrillar organic matrix comprises a total of ~10%, and again within this group of proteins, osteocalcin and osteopontin are present in a large proportion (1 to 2% in a healthy bone). Together with collagen, these noncollagenous matrix proteins form a scaffold for hydroxyapatite deposition. Osteocalcin and osteopontin have recently begun to be recognized as critical determinants of bone quality and its ability to resist fracture (1–7). Besides osteocalcin and osteopontin, a few other abundant noncollagenous bone matrix proteins have been identified such as fibronectin, osteonectin, bone sialoprotein II, decorin, and bioglycan (8, 9). The remaining noncollagenous proteins of bone matrix include proteases, bone morphogenetic proteins and growth factors (10). Bone matrix quality varies with age, nutrition, disease, and anti-osteoporotic treatments (11–14) and is known to be a major contributor of post-yield deformation and fracture of bone (15). As low bone mass alone is insufficient to cause fragility fractures (16), factors other than the loss of bone mass such as changes in the quality of bone matrix proteins and their modifications are of crucial importance to the understanding and prediction of fragility fractures (17).

Bone fractures are the leading cause of serious health problems, especially in elderly population. The link between bone quality and public health is well understood but bone analyses are also very important to other research fields than medical sciences. For example, bone preserves the entire protein pattern of extracellular bone matrix proteins for thousands of years. It was shown that the profile quality of the matrix proteins isolated from ancient bones is similar to the profile from bones harvested recently (18). Because of such exceptional preservation of bone proteins quality, recent paleoanthropological studies linked differences in amino acid sequence of osteocalcin to nutritional habits of Neanderthals, primates, and modern humans (19). Most often, analyses of bones are limited by the amount of available material. In addition, bone is a highly heterogenous tissue, and the ability to microdissect homogenous parts under direct microscopic

visualization could help to identify structural and metabolic variations within individual bones.

Laser capture microscopy (LCM)[1] is a powerful technology that can supply exceptionally pure samples for studies employing various analytical techniques (20). Originally, LCM was developed for dissection of soft biological materials (21) such as a specific group of cultured osteobalsts (22), cells from mice intervertebral discs (23), odontoblasts from biodegradable polymer scaffolds (24), cranial neural crest mesenchyme (25), dental follicle, and surrounding mandibular bone of newborn rats (26). Notably, a skeletal tissue of newborn mice (27) was also dissected using LCM. However, skeletal tissue of newborn mice is known to be not fully mineralized up to 3–4 weeks after birth (28, 29), and thus, cannot be compared with laser microdissection of a cortical bone of an adult human. We thought, if sufficiently thin, human cortical bone slice could be bound to a membrane, cut with a laser and a single-piece structural bone component could be used for a number of biochemical analyses.

In adult vertebrates, bones are constantly renewed by remodeling, which comprises highly regulated bone resorption and formation processes. The remodeling processes change over a life-time and influence the amount of bone mass in a body. Imbalance between bone resorption and formation leads to osteoporosis, the most frequent degenerative condition of bones characterized by a low bone mass and low bone quality (30). It is also thought that mechanical strain plays an important role in adaptive responses of bone. In particular, when loading conditions are perturbed, mechanical strain levels define the thresholds for remodeling activity in normal bone (31). One may assume that strain histories differ between regions of the same bone and as such, through remodeling processes bone should be able to adjust its structural/material organization in response to regional heterogeneities. Consequently, the changes in bone remodeling processes would be reflected by the relative differences between osteonal (younger) and interstitial (older) bone tissue. For this reason we selected these two types of bone tissue for our study.

Age-related changes in abnormal bone remodeling are primarily associated with diminishing quality of collagen because of undesired glycation, the process that results in chemical modifications of proteins by carbohydrates (32, 33). Pentosidine (PEN) represents nonenzymatic, pentose-derived crosslink formed between lysine and arginine residues of collagen and is used as a biomarker for cumulative nonenzymatic glycation damage to proteins. Pyridinoline (PYD) and deoxypyridinoline (DPD) are mature trivalent crosslinks that play an important role in stabilization of collagen fibers *in vivo*. Because of their clinical importance, we selected PEN as the primary representative of advanced glycation end products (AGEs) and PYD and DPD, two enzymatic posttranslational modifications of collagen, as model crosslinks in our current studies. It is noteworthy that all three compounds are naturally fluorescent and difficult to quantify because of their very low concentrations in bone and serum. To assess differences between osteonal and interstitial bone tissue with the respect to the aforementioned collagen crosslinks, we chose ultra-high-performance liquid chromatography (UPLC) over high-pressure liquid chromatography (HPLC), because UPLC has much higher sensitivity and allows fast analysis of nanoscale sample amount. However, the UPLC system was not used for AGEs quantification before, thus first, it was necessary to develop the appropriate methods.

Here, for the first time we present a strategy that enables in-depth biochemical analyses of nearly nanoscale amounts of exceptionally homogenous bone tissue. Using laser-capture microscopy instead of mechanical milling (34), we developed capabilities for microdissecting human cortical bone pieces of 0.00014 mm^3 (or less) in size. This experimental procedure allowed us to dissect osteonal and interstitial bone tissues of outstanding purity and perform comprehensive biochemical analyses of their matrix proteins. We used our newly developed separation methods and two-dimensional SDS-PAGE combined with matrix-assisted laser desorption ionization/time of flight (MALDI-TOF/TOF) MS and tandem MS (MS/MS) to analyze bone-matrix proteins from 24 osteonal and 24 interstitial tissue pieces of a cadaveric donor (76 years old Caucasian female). Our results show that collagen in older interstitial tissue contains higher levels of PEN ($p < 0.0001$) and two enzymatic crosslinks (PYD, $p < 0.001$ and DPD, $p < 0.001$) than younger osteonal tissue. Although our data on PYD and DPD levels agree with the ones reported by others, our results on PEN levels are opposite (34) and suggest a link between accumulation of glycation-derived crosslinks and normal aging of generally healthy subjects. Conversely, osteonal tissue has higher amount of osteopontin and osteocalcin than interstitial tissue, and this has not been demonstrated before. Taken together, these data show statistically relevant differences between younger osteonal and older interstitial bone tissue at the level of three major bone matrix proteins, collagen, osteocalcin, and osteopontin. We propose that our results have important implications for bone remodeling and microdamage formation, as due to the altered amount and quality of the aforementioned matrix proteins the bone's hierarchical microarchitecture would become markedly affected. Moreover, as our strategy allows in-depth analysis of

[1] The abbreviations used are: LCM, laser capture microscopy; UPLC, ultra-high pressure liquid chromatography; MALDI TOF/TOF MS (MS/MS), matrix-assisted laser desorption ionization tandem time-of-flight mass spectrometry; LCMD, laser capture microdissection; PEN, pentosidine; PYD, pyridinoline; DPD, deoxypyridinoline; AGEs, advanced glycation end products; EDTA, 2,2′,2′′,2‴-(ethane-1,2-diyldinitrilo)tetraacetic acid; Tris-HCl, 2-amino-2-(hydroxymethyl)-1,3-propanediol hydrochloride; OPN, osteopontin; OC, osteocalcin; ELISA, enzyme-linked immunosorbent assay; INT-PYD, acetylated pyridinoline; ATW buffer, (acetonitrile:trifluoroacetic acid: water) buffer.

very limited amounts of bone material, it can also be useful in such fields as forensic, anthropology and archaeology.

EXPERIMENTAL PROCEDURES

Laser Capture Microdissection of Bone Tissues—Human cortical bone (posterior quadrant) specimens obtained from a cadaveric donor (76 years old Caucasian female; purchased from the centralized National Disease Research Interchange biobank) were embedded in poly-methyl methacrylate and sectioned transversely (*i.e.* perpendicular to its long axis) into 5 μm thick sections. Sections were bonded to a membrane slide (Molecular Machines and Industries (MMI), Haslett, MI) using 70% ethanol, which was carefully brushed onto the membrane using a soft-tipped paintbrush to avoid formation of air bubbles, and then dried. In the next step, the boundaries of the slide were configured and pre-imaged to locate and orient the bone specimen on the slide using the Olympus IX71 Inverted Microscope (Olympus America Inc., PA). This microscope was equipped with MMI CellTools (Version 3.48, MMI, Eching, Germany) software that also automatically calculated the surface area of the cut bone piece. Based on the image displayed on the computer screen at 20× magnification and under a regular bright light, osteonal and interstitial regions as well as random areas of bone were selected for cutting. Each laser-cut bone tissue was automatically collected on an adhesive cap of a tube (MMI) positioned in a holder above the slide. The laser (335 nm) speed, focus and power (*e.g.* 15%, 30%, and 90%) were selected according to the thickness of the samples. Five laser cuts were used to cut 5 μm bone slice. The volume of each sample was calculated using the surface area and bone-piece thickness of 5 μm. The samples (total of 24 LCM dissected osteonal, 24 interstitial, and 38 random bone pieces) were used immediately for protein isolation or stored at −80 °C until use.

Protein Isolation—Previously used methods for isolation of proteins from large-size bone samples (35, 36) were modified for the processing needs of the LCM dissected bone pieces. Thus, the extraction buffer (0.05 M EDTA, 4 M guanidine chloride, 30 mM Tris-HCl, 1 mg/ml bovine serum albumin, 10 μl/ml Halt Protease Inhibitor (Pierce, Waltham, MA) pH 7.4) was added directly into the tubes containing microdissected samples that were to be used for enzyme-linked immunosorbent assay (ELISA) experiments. The samples to be used for gel electrophoresis were prepared in the buffer containing 15% glycerol (ultrapure, HPLC/spectroscopy grade) instead of bovine serum albumin. The tubes were incubated overnight on ice in inverted orientation to facilitate detachment of a given bone piece from the adhesive cap. In the next step, one to five solutions (this depended on the type of the performed experiment) containing one bone piece were transferred into an eppendorf tube that had a hole melted in the lid. The tube was covered with a dialysis membrane (Spectra Por® 3 Dialysis Membrane; Spectrum Laboratories, Inc., Gardena, CA) and closed allowing the membrane to line the hole. Simultaneous protein isolation and demineralization was performed using micro-dialysis at 0–2 °C against several changes of the phosphate-buffered saline buffer, pH 7.4. This approach significantly shortened the process of protein isolation as compared with the standard procedures for the isolation of proteins from bone matrix (11, 35, 36) and significantly lowered the likelihood of protein degradation. After micro-dialysis, the samples were centrifuged. Collagen pellets were used for determination of selected crosslinks. These pellets contain collagen modified by different types of crosslinks as opposed to the soluble collagen fibers that are newly synthesized and serve as the substrates for crosslinking (37–39). After the measurement of protein concentration, supernatants were either used directly for two-dimensional SDS-PAGE (*i.e.* supernatants contained an equal (~250 ng) total-protein contents), osteopontin (OPN) and osteocalcin (OC) ELISA analyses or freeze-dried and stored at −80 °C until use.

Determination of Pyridinoline, Deoxypyridinoline, and Pentosidine Crosslinks of Collagen—Sample hydrolysis of the microdissected bone tissue (pieces of 0.00014 to 0.00015 mm^3 in size) and collagen pellets was performed in 20 μl of 6N HCl at 110 °C for 20 h. The hydrolysates were freeze-dried and then dissolved in 30 μl of 1% n-heptafluorobutyric acid. PYD, DPD, acetylated pyridinoline (INT-PYD, *i.e.* internal standard), and PEN were separated using an Acquity UPLC machine (Waters Corp., Milford, MA) equipped with the Acquity UPLC HSS T3 column (1.8 μm; 2.1 × 100 mm). The column flow rate and temperature were 0.667 ml/min and 40 °C, respectively. Gradient of 10 to 31% of Solvent B was used for the separation of the collagen crosslinks. Solvent A consisted of 0.12% n-heptafluorobutyric acid in 18 ohms pure water, and solvent B was composed of 50:50 (v:v) mixture of solvent A : acetonitrile. Prior to use, the column was equilibrated using 10% solvent B. The elution of PYD, DPD, and INT-PYD was monitored for fluorescence emission at 395 nm after excitation at 297 nm. PEN was monitored for fluorescence emission at 385 nm after excitation at 335 nm. Standard curve was used to quantify PEN. After each analysis, the column was washed using 95% acetonitrile for 1 min and equilibrated with solvent A.

Statistical analyses of the determined PYD, DPD, and PEN contents in osteonal, interstitial, and random bone pieces were performed according to the standard *t* test.

Determination of Collagen Contents—Sample hydrolysis of the microdissected bone tissue (pieces of 0.00014 to 0.00015 mm^3 in size) and collagen pellets was performed in 20 μl of 6N HCl at 110 °C for 20 h. Hydroxyproline content was determined using reagents from the HPLC assay kit (Bio-Rad Laboratories GmbH, Munchen, Germany). The 0 to 50% gradient of acetonitrile was achieved by mixing 100% acetonitrile with a buffer composed of 0.3% acetic acid and 0.6% triethylamine, pH 4.50. The amount of hydroxyproline was calculated assuming 300 nmol of hydroxyproline in 1 mol of collagen.

Hierarchical Separation of Bone-matrix Proteins Using Two-dimensional SDS-PAGE—The two-dimensional SDS-PAGE is based on standard (8 cm × 8 cm) polyacrylamide gels (thickness of 1 mm or less) and small-size apparatuses instead of large ones that are difficult to handle and require much more toxic reagents. Separation of protein extracts was conducted using the NuPAGE gels (NuPAGE Technical Guide IM-1001, version E; Invitrogen, Carlsbad, CA, USA). Gel staining and preparation of proteins after their cutting from the gel was performed according to the protocols included with the "SilverQuest" silver staining kit compatible with mass spectrometry (Invitrogen). The "Silver Express" staining kit was also tested to determine its applicability with chymotrypsin digestion, and thus, for the generation of peptides for MALDI-TOF/TOF MS analysis. Silver-stained protein spots as well as gel area free of proteins were cut out from the gel and processed before enzymatic digestion according to the procedures described by Gharahdaghi *et al.* (40) which also include methods for removal of silver ions, in-gel protein reduction and alkylation.

Sample Preparation for MALDI-TOF/TOF MS—In-gel enzymatic digestion of proteins was conducted according to the protocols included with trypsin (Promega, Madison, WI) and tosyl-L-lysine chloromethyl ketone treated mass-spectrometry grade chymotrypsin endoproteinase (Thermo Scientific, Rockford, IL). Peptide mixtures were desalted and purified using C18 solid phase extraction pipette tips (PerfectPure C18 Tips, Fisher Sci., Pittsburgh, PA). Each C18 column tip was conditioned once with 10 μl of the acetonitrile:trifluoroacetic acid:water (ATW) buffer (50% acetonitrile/0.1% trifluoroacetic acid mixture in water) and then three times with 10 μl of 0.1% trifluoroacetic acid/water solution. In order to bind peptides to the C18 column, 5–10 μl of each sample were passed three times through the column. Subsequently, the column was washed three times with 5–10 μl of 0.1% trifluoroacetic acid. The peptides were eluted using 5 μl of

the ATW buffer and used directly for MALDI-TOF/TOF MS analysis or stored in −80 °C until use.

MALDI-TOF/TOF MS—Approximately 1 μl of matrix α-cyano-4-hydroxycinnamic acid was spotted on the MALDI plate followed immediately by ~0.5 μl of the sample to ensure even mixing with the matrix before drying. All spots were prepared in duplicates for each specimen, and all samples on the plate were completely dried before MALDI analysis. Mass spectrometry was performed on the Ultraflex III MALDI-TOF/TOF (Bruker Daltonics) equipped with a smartbeam nitrogen laser (337 nm, UV) in positive ion reflection mode. Twenty laser shots were averaged to create a single spectrum with a high-signal to low-noise ratio. All data were acquired in a linear mode. FlexAnalysis Version 3.0 (Bruker Daltonics) software was used for spectrum acquisition and analysis. The average *m/z* values for the peaks were identified automatically by the software. Detailed composition of the *m/z* values for each averaged peak was determined manually (supplemental Fig. S3, S4 and S5). In the next step, peptide ionization of the selected peaks was performed. Depending on the *m/z* value of a given peptide peak, the corresponding MS/MS fragmentation scan was conducted from *m/z* 100–1000 for the peptide with *m/z* 965.50, from 100 to 1100 for the peptide with *m/z* 1020.41, from 100 to 1200 for the peptide with *m/z* 1180.63, from 100 to 2000 for the peptide with *m/z* 1854.90, etc.

Spectra Analysis—In conjunction with mass spectrometry experiments, proteomics tools (Protein Prospector) available through the University of California, San Francisco (http://prospector.ucsf.edu/prospector/mshome.htm) for mining sequence databases, were used to identify proteins based on *m/z* values of the peptides and fragment ion data. Submission of the peptide *m/z* data to the SwissProt.2008.0610/NCBInr.2008.11.25 database was performed through the MS-Fit program of Protein Prospector following the online instruction. Submission of the fragment ion data (collected after ionization of the detected peptides to SwissProt 57.11) was performed through the MS-Isotope program (linked to MASCOT MS/MS search tool) following the online instruction. The searched database of SwissProt 57.11 covered 512,994 sequences, which correspond to 180,531,504 residues. The searched human database subset of SwissProt 57.11 covered 20,401 sequences. The MASCOT MS/MS search parameters included monoisotopic mass values, ± 0.3 Da peptide mass tolerance and ± 0.5 Da fragment mass tolerance. The Mascot Score Histogram was –10*Log(P), where P is the probability that the observed match is a random event. Individual ions scores >19 indicated peptides with significant homology (*e.g.* human OPN score was 21; page 51 of supplemental Data). Protein scores were derived from ions scores as a non-probabilistic basis for ranking protein hits. The employed threshold score/expectation values facilitated clear distinction between the top-protein hit (*i.e.* score of 21 for human OPN) and the remaining protein hits (*e.g.* the next highest score of 6 was for human LIM domain kinase 1 and this protein was excluded).

Enzyme-Linked Immunosorbent Assays (ELISAs)—Detection and quantitation of OC and OPN were performed according to the protocols included with the hOST-EASIA and Human Osteopontin Assay kits (ARP American Research Products, Inc., Belmont, MA).

RESULTS AND DISCUSSION

To address the needs of bone research, we developed a strategy permitting comprehensive biochemical characterization of major bone-matrix proteins using nanoscale-size bone samples and proteomics methodology. The strategy was applied to the analysis of protein levels and protein modifications of bone matrix to facilitate our investigations on their potential links to bone remodeling and fragility fractures.

Laser Capture Microdissection of Bone Tissue—This procedure was performed on mineralized bone specimens which were embedded in a polymer (*i.e.* poly-methyl methacrylate). Thus both, bone's microcrystalline mineral and the polymer were protecting proteins from degradation by preserving, for example, their spatial separation and structural organization. Moreover, it has been shown that bone preserves extracellular matrix proteins over thousands of years and this capability was also observed for bones excavated at room temperature (41). Therefore, we assumed that bone matrix proteins in modern bones, which were used in our studies, should represent a good quality profile, especially with all precautions taken to preserve these as well as possible. To bond bone samples onto an RNase free, 1.4 μm thick polyethylene terephthalate membrane slide from MMI, we selected 5 μm thick sections of human (cadaveric 76 years old Caucasian female donor) cortical bone beams. Nanopure water alone, a 0.1% poly-L-lysine solution, 0.1% agarose solution as well as 70% ethanol solution were tested for bonding efficiency. Incubation of the samples using 70% ethanol solution supplied the best quality samples that withstood multiple laser cuts. A clear advantage of using a solution of volatile ethanol is the lack of introducing of any additional chemical compounds to the samples. Even in small concentrations, such undesired compounds can interfere with enzymatic digestion and dominate mass spectra because of the ease of ionization and much greater amount when compared with amounts of single peptides. Our next goal in adapting the LCM for microdissection of mature, fully mineralized bone was to determine the optimal cutting parameters for laser, which included laser's speed, focus and power. Optimal parameters should facilitate efficient bone cutting, but they should not lead to overheating of the bone section close to the line of cutting (20, 21). We established that selecting the laser speed at 13 to 15%, focus at 30 to 45% and power at 90% was optimal to dissect a bone piece of 0.00014 to 0.00015 mm^3 in size after five laser shoots. Commonly, bone sections are not evenly thick (the difference approx. 0.05 μm) and this was the case for the tested 5 μm thick human cortical bone samples. Thus, we also established that one laser shoot was sufficient to dissect the thinner bone parts, whereas the thicker parts required up to eight laser shoots. As the majority of the cut out bone structures required five laser shoots, we concluded that they corresponded to 5 μm thick human cortical bone sections and used only the five-laser-shoots sections to avoid potential variation caused by thickness difference between the dissected bone pieces. The procedure developed for microdissection of random bone pieces was then applied for cutting osteonal and interstitial bone tissue (Fig. 1*A* and *B*).

Minimal Number of Bone Pieces Required for Each Analysis—The amount of the LCM dissected bone tissues that are on the interface of micro- and nanoscale impose various constrains onto the experimental work. Therefore, we conducted a cumulative moving average analysis (42) to deter-

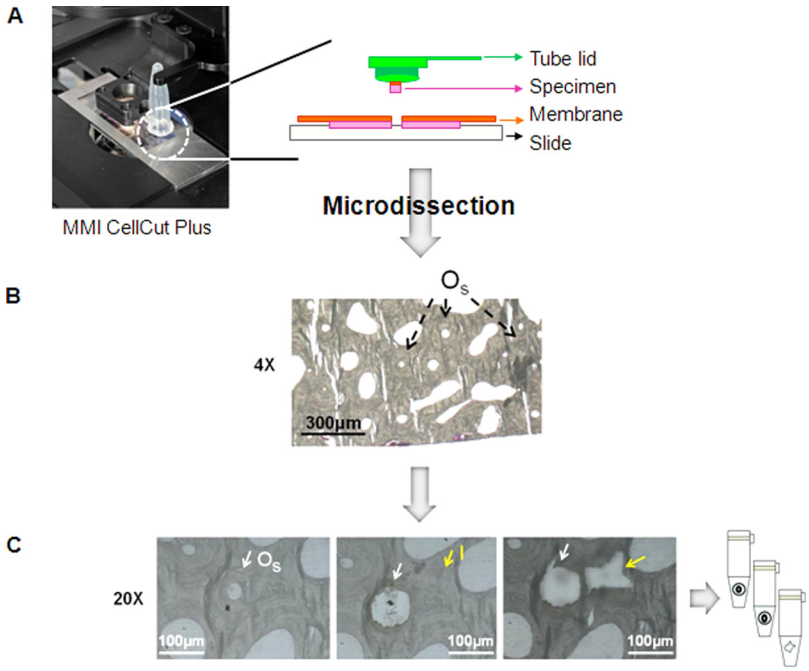

FIG. 1. **Schematic showing the principle of bone tissue microdissection using laser capture microscopy and its application.** *A*, Collection of a sample through the adhesive cap of an eppendorf tube. *B*, Image of the human cortical bone section shown under 4× magnification. The arrows show the areas with secondary osteons (O_s). *C*, images of the human cortical bone section shown under 20× magnification. Images represent examples of microdissected osteonal (O_s, white arrow) and interstitial (I, yellow arrow) bone tissue before (*left*) and after (*right*) collection of the samples. The empty areas are left behind after collection of a given bone piece and this is also one of the LCM tests demonstrating that a given bone sample was indeed captured by the sticky lid.

mine the minimal number of bone pieces required for each experiment using randomly microdissected bone tissue. The random bone pieces comprised of a mixture of osteonal and interstitial regions that were either distant from osteons or were located close to the edge of the 5 μm thick human cortical bone beams. Four batches of samples contained 1, 3, 5, or 7 bone pieces, respectively. Each piece was 0.00014 to 0.00015 mm^3 in size. Notably, detection of the selected enzymatic mature (PYD, DPD) and nonenzymatic (PEN) crosslinks of collagen as well as hydroxyproline using UPLC was possible even when using one bone piece of 0.00014 to 0.00015 mm^3 in size. However in this case, the work was conducted near the detection limit, and as a consequence, a larger number of the single-piece samples was required to collect reliable data. Based on the cumulative moving average analysis, we established that the minimal number of the laser microdissected bone pieces required for all UPLC analyses to be done on one sample batch would be five pieces (0.00070 to 0.00075 mm^3 in size) (supplemental Fig. S1). In contrast, two to three pieces (0.00028 to 0.00045 mm^3 in size) were sufficient for two-dimensional SDS-PAGE. This amount facilitated detection of the qualitative differences between osteonal and interstitial subproteomes whereas permitting the collection of spots of interest for MALDI-TOF/TOF MS analysis. The work on determination of the minimal number of bone pieces required for each analysis was motivated by its fundamental importance to discovery and nonquantitative identification of bone-matrix biomolecules.

New UPLC Methods for Determination of Naturally Fluorescent Collagen Crosslinks—To determine the contents of fluorescent enzymatic mature (PYD, DPD) and nonenzymatic (PEN) crosslinks of collagen, we developed new UPLC methods that differ from conventional HPLC methods (43, 44) as well as our separation methods developed recently for proteins and large bone pieces using Acquity UPLC machine (45). The first difference refers to sample pretreatment. According to the standard HPLC approach, the hydrolyzed bone samples need to be cleaned before separation using prepacked solid phase extraction Chromabond® Crosslinks columns (43). We established that pretreatment of the samples using solid phase extraction columns was unnecessary in the case of LCM dissected bone tissues. We found that the quality of the UPLC separation was similar for the samples that were prepared by 6N HCl hydrolysis of collagen extracted from the LCM-dissected bone pieces and the samples that were directly hydrolyzed using 6N HCl. Although the pretreatment on the solid phase extraction columns is not required for analyses performed on purified collagen, the lower contents of interfering fluorescent compounds in directly hydrolyzed bone samples by our protocol could probably be attributed to the exceptional uniformity observed among the randomly chosen osteonal and interstitial bone pieces. The second fundamental difference between the conventional HPLC and our UPLC methodology is the use of one-column-type, but different separation conditions, for all the analyses. Standard HPLC methods used for separation of collagen's PYD, DPD, and PEN combine isocratic separation of PYD and DPD, and gradient separation for elution of PEN. We determined that isocratic separation was unsuitable for separation and detection of PYD and DPD using UPLC (no peaks were detected in the designated time-frame). Although PEN was detected, its retention times were four- to fivefold shorter than the ones described in the literature (43, 44). Introduction of a single,

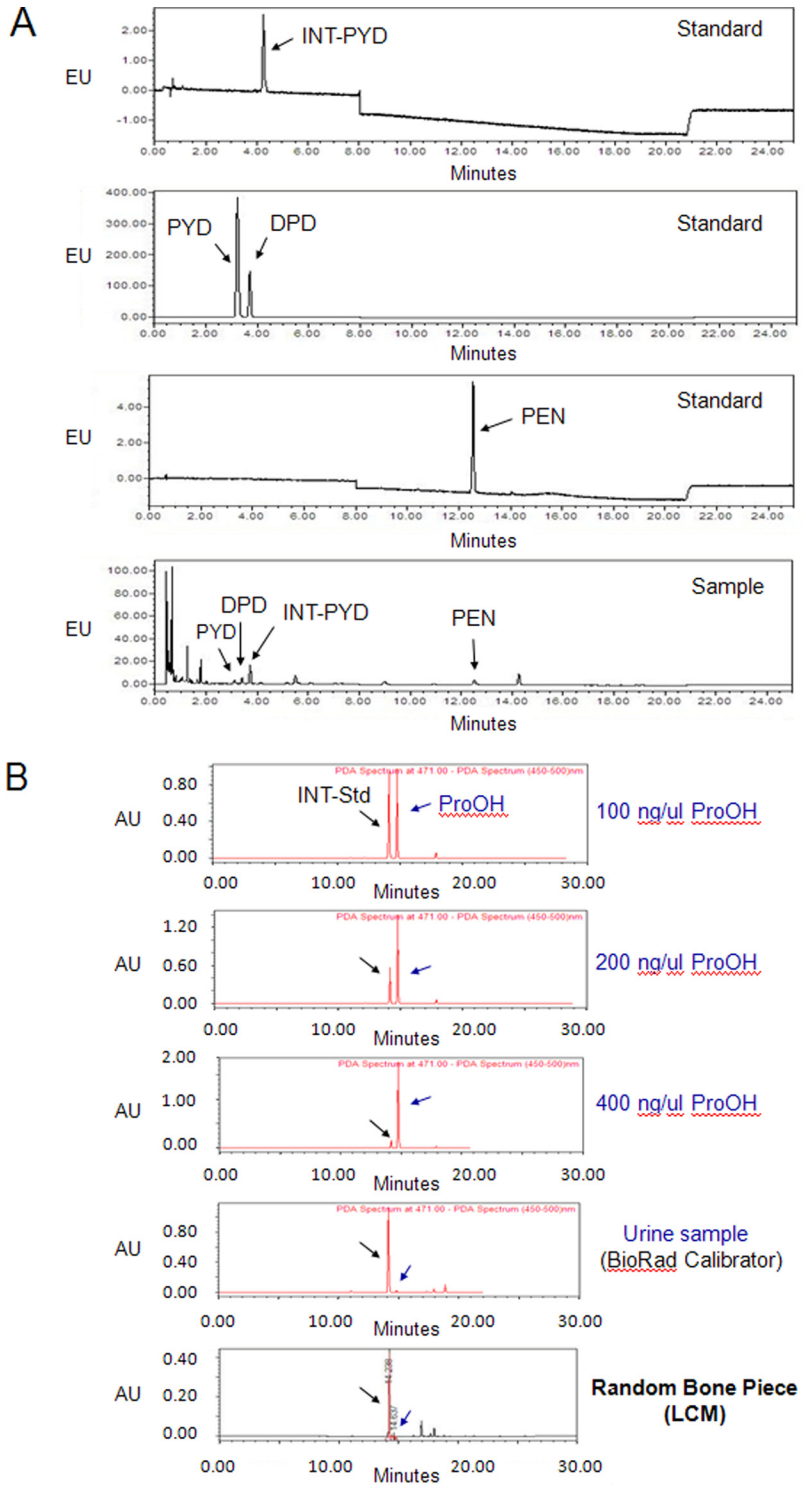

FIG. 2. **Examples of the UPLC chromatograms.** *A*, Chromatograms showing separation of the INT-PYD, PYD, DPD, and PEN standards (first three panels) and detection of PYD, DPD, and PEN in the HCl-hydrolyzed random laser-microdissected bone tissue (Sample). The identified cross-links are described directly in the figure. *B*, Chromatograms demonstrating separation of the derivatized hydroxyproline (ProOH) and internal standard (INT-Std) from ProOH solutions, BioRad calibrator and LCM dissected bone tissue using the same column as for the separation of the three collagen crosslinks but different separation conditions.

relatively broad (10 to 31%) separation gradient led to consistent separation of PYD, DPD, acetylated pyridinoline (internal standard), and PEN (Fig. 2*A*).

Our UPLC method for separation and determination of hydroxyproline in bone samples also has several unique features. First, we use the Acquity HSS T3 column instead of the commonly used Bio-Rad Analytical 195–9520 column (43). Thus, detection and determination of hydroxyproline (to determine collagen concentration by assuming 300 nmol hydroxyproline in 1 mol of collagen) is achieved on the same type of column as the selected collagen crosslinks (Fig. 2*B*). Ability to perform all the separations using one type of column, but different separa-

tion conditions, is of fundamental importance to fast and simple quantification of collagen crosslinks. It is also less expensive as additional types of columns are not required. Second, we do not use the Bio-Rad solvents for the elution of derivatized hydroxyproline as the respective solvents were developed for classical HPLC separation on a different column type. Our solvents are composed of acetic acid, triethylamine, and acetonitrile. We achieved optimal separation of the derivatized hydroxyproline under gradient conditions when low pH (4.30 to 4.50) solvents were used. The immediate application for the methods developed in our study can be, for example, a subproteome/proteome-scale analysis of glycation end-products of bone-matrix proteins. More broadly, applications of the discussed UPLC separation methods can go beyond medical sciences as they allow in-depth analysis of very limited amounts of bone material.

Hierarchical Separation of Bone-matrix Proteins Using Two-dimensional SDS-PAGE—For work in the area of proteomics, a procedure for hierarchical separation of bone-matrix proteins using one- and two-dimensional SDS-PAGE was introduced. It facilitates stepwise separation and visualization of very small amounts of protein samples originating from LCM microdissected bone tissues (Fig. 3*A*, *B*, and *C*). We use the term "hierarchy" to describe separation of bone-matrix proteins that differ significantly in their abundance in bone. The amount of organic matrix in bone varies with age, state of maturation and turnover, skeletal location, diet, and health, but it is generally 10 to 30% of a bone. Of our particular interest were collagen (~90% of total bone matrix proteins), osteocalcin (OC) and osteopontin (OPN) (each 1 to 2% of total bone matrix proteins) (46), because our preliminary work established that the quality and the amount of these three major bone matrix proteins has a significant influence on the quality of bone's microcrystalline phase, bone's mechanical properties and resistance to fracture at micro- and macro-scale (13–15, 47). This is why in this part of our research, we focused on the second pool of the most abundant bone matrix proteins and determination of potential differences between the corresponding pools (also termed subproteomes) originating from osteonal and interstitial tissue. Notably, it was demonstrated by immunocytochemistry that OC and OPN are indeed present in the targeted tissue compartments (48).

Using hierarchical separation approach, we first identified and collected ultrapure collagen samples (for other studies than discussed here) using one-dimensional SDS-PAGE (the first protein pool, Fig. 3*A* and supplemental Fig. S2), whereas osteocalcin, osteopontin and a few other non-collagenous bone matrix proteins were separated in the second dimension SDS-PAGE (the second protein pool, Fig. 3*A*, *B*, and *C*). We think that the hierarchical protein separation approach using different two-dimensional SDS-PAGE techniques can serve as particularly useful tool to investigate variation and/or changes in the most abundant pools of bone proteins when a very limited amount of bone sample is available, or more broadly, to study other systems with hierarchically abundant

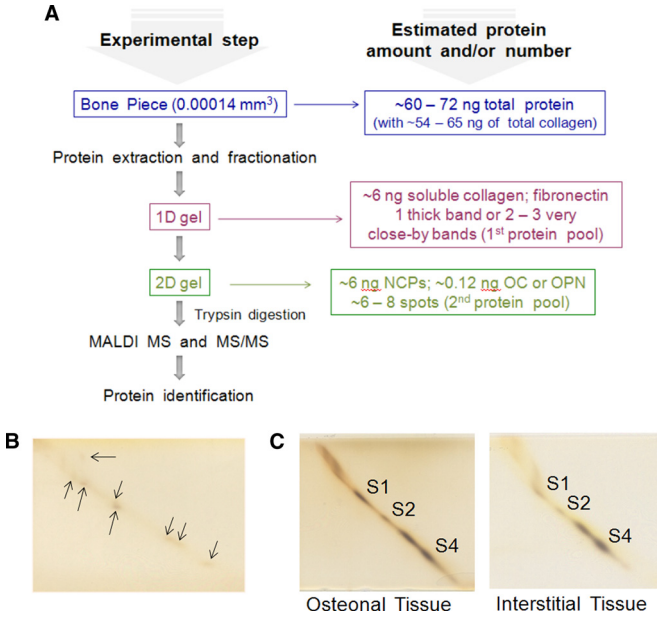

FIG. 3. **Work flow for hierarchical separation of the major bone-matrix proteins discussed in this paper.** *A*, The estimated total amount of recovered proteins is shown at the corresponding experimental step. *B*, The method used for protein isolation was providing six to eight major NCPs that are critically involved in bone's resistance to fracture in as little as ~50 ng of the total protein extract used for the separation in the first SDS-PAGE dimension. Notably, the remaining pool of NCPs can be accessed at the next separation step (to be published elsewhere). Abbreviation MW, molecular weight marker; Novex Sharp Protein Standard (Invitrogen, Hercules, CA). *C*, The two-dimensional SDS-PAGEs showing separation of the second most abundant pool of NCPs from osteonal and interstitial tissue of a human cortical bone pieces (76-year-old cadaveric Caucasian female donor). Equal amounts of protein extracts (~250 ng) that corresponded to three bone pieces were loaded onto one-dimensional SDS-PAGE. These amounts corresponded to the total protein content present in the three bone pieces dissected using LCM. Protein spots selected for MALDI-TOF/TOF MS analysis (S1, S2, and S4) are marked directly on the gel images.

proteins such as certain specialized cells (*e.g.* mammary epithelial cells) and tissues (*e.g.* egg-shell matrix proteins) of endangered species. Notably, for bone samples available in larger amount, the remaining bone matrix proteins can already be detected and analyzed at the second separation step when using this approach.

To investigate potential qualitative and quantitative differences between osteonal and interstitial bone tissue at the second sub-proteome level, we combined two-dimensional SDS-PAGE with MALDI-TOF/TOF MS. Analysis of the selected protein spots using MALDI-TOF/TOF MS and MS/MS was performed after in-gel enzymatic digestion followed by peptides' mixture purification. Specifically, we applied our newly developed analytical methods to investigate the selected collagen crosslinks and bone-matrix proteins in extremely uniform samples of LCM-dissected osteonal (24 bone pieces from 76 years old cadaveric Caucasian female donor) and interstitial (corresponding 24 bone pieces from the same

TABLE I

Quantitative analysis of crosslinks in laser-microdissected bone (human, cortical) tissues. Statistical analysis (t-test) showed significant differences in PYD, DPD, and PEN with tissue age (i.e., osteonal being young and interstitial being old). There is a greater amount of PYD/collagen ($p < 0.001$), DPD/collagen ($p < 0.001$), and PEN ($p < 0.001$) in interstitial tissue compared to osteonal tissue

Sample	Collagen [nmol/mm^3 of bone]	PYD [mmoles/mol collagen]	DPD [mmoles/mol collagen]	PYD/DPD ratio	PEN [mmoles/mol collagen]
Osteon	0.526 ± 0.090	28.54 ± 3.49	23.146 ± 9.02	1.23	0.011 ± 0.002
Interstitial	0.498 ± 0.092	111.901 ± 13.69	164.298 ± 64.99	0.68	6.028 ± 1.22
Random bone piece	0.368 ± 0.099	88.77 ± 10.86	158.583 ± 62.74	0.56	1.72 ± 0.35

cadaveric donor) bone tissue. There were several reasons for selecting this particular donor and the key ones are as follows. Generation of AGEs, in particular pentosidine, is time-dependent and AGEs tend to accumulate with aging (49). However, it has been unclear why a newly formed osteonal bone tissue formed in old and middle-age donors was reported to show the opposite trend (34). We thought that our experimental strategy can elucidate this unusual phenomenon.

Lower Level of Fluorescent Crosslinks in Younger Osteonal Bone Then Older Interstitial Bone—First, we showed that collagen crosslinks quantified in LCM microdissected bone tissues using the developed UPLC methods were within the same range (mmoles/mol collagen) as those quantified from larger bone pieces of 20 mg or more in weight (50) and macro-cores of osteonal and interstitial tissue (mechanically milled and weighted on microbalance) (34) using standard HPLC protocols. Next, we determined that the amounts of PYD and DPD in osteonal bone were lower (~4- to 4.5-fold) than the corresponding amounts in the interstitial bone tissue (Table I). The PYD level was higher than DPD and resulted in larger than 1 PYD/DPD ($R_{PYD/DPD} > 1$). Conversely, interstitial bone tissue and samples of random bone pieces showed slightly elevated levels of DPD over PYD. In agreement with the age difference of the analyzed tissue (*i.e.* osteonal being young and interstitial being old), the total amounts of PYD and DPD were lower in osteonal than in interstitial tissue. Our PYD/DPD data agree with those reported for whole bone (51, 52) and large osteonal and interstitial bone cores (34); however, the best comparison can be made with data on large osteonal and interstitial bone cores (34). Similarly higher PEN levels, which correspond to tissue aging, were observed in the older (interstitial) bone tissue and all the data were statistically significant (Table I). Thus, we established that collagen in older bone tissue contains higher levels of the advanced glycation end product PEN and other crosslinks. This observation is contrary to the published data that showed the opposite trend, specifically, significantly higher PEN levels in younger osteonal than older interstitial tissue from old and middle-age donors (34). Such discrepancy might have arisen from using larger bone pieces as compared with our samples, which not only may contain more osteons but also their populations may be more diversified. Therefore, we concluded that our samples contained populations of osteons of similar tissue age with similar levels of collagen crosslinks. Importantly, our data comply with the mechanism and time-frame of PEN formation in long-lived tissues (32) as well as our previous work showing that accumulation of nonenzymatic glycation end-products in cortical bone causes stiffening of the type I collagen network in bone, and thus, may explain some of the age-related increase in skeletal fragility and fracture risk (33). Thus, here, not only we show the power of the developed UPLC methods but their potential for applications in, for example, medicine, forensics, archaeology, and anthropology where bone samples can be very small and precious.

Identification of Differences Between Major Matrix Proteins From Osteonal and Interstitial Bone Tissue—The two-dimensional SDS-PAGE analysis revealed several differences between osteonal and interstitial bone tissue at the second sub-proteome level (Fig. 3*C*). To demonstrate the power of the developed methodology, three spots that clearly differed, were selected for identification using MALDI-TOF/TOF MS and MS/MS. As we used two different silver staining kits, one compatible and the other one not compatible with trypsin digestion, protein spots were digested either with trypsin or chymotrypsin. Identification of proteins was based on triptic instead of chymotriptic digest because of a larger number of peptides identified from triptic digests (supplemental Table S1 and S2). For example, in the case of protein spots S1 and S2 (Fig. 3*C*), MALDI mass spectra of tryptic digest were dominated by the ions with *m/z* 965.50, 1020.41, 1180.63, and 1854.90 (Fig. 4*A*, *B*). The MALDI mass spectra of chymotrypsin digest were dominated by the ion with *m/z* 1621.93 (55–69 AAs, LAPQNAVSSEETNDF) suggesting that the enzyme had access to this region of the crosslinked protein. Submission of the *m/z* data (tryptic digests) to a Protein Prospector (UCSF, San Francisco, CA) search of the SwissProt.2008.06.10 database yielded a match to peptides of human osteopontin precursor (Pre-OPN) for protein peptides derived from the S1 and S2 spots (supplemental Table S2 and page 11 to 31 of supplemental Data). As mobility of osteopontin in PAGE depends on the degree of its modifications, these results explain the detection of OPN in the two spots. In contrast, the MALDI mass spectra of the tryptic digest of the S4 spot were dominated by the presence of the ions with *m/z* 875.44 (40–47 AAs, QEGSEVVK), 1267.68 (40–50 AAs, QEGSEVVKRPR), 1535.799 (33–47 AAs, GAAFVSKQEGSEVVK), and 2274.20 (52–70 AAs, YLYQWLGAPVPYPDPLEPR). Submission of the *m/z* data to a

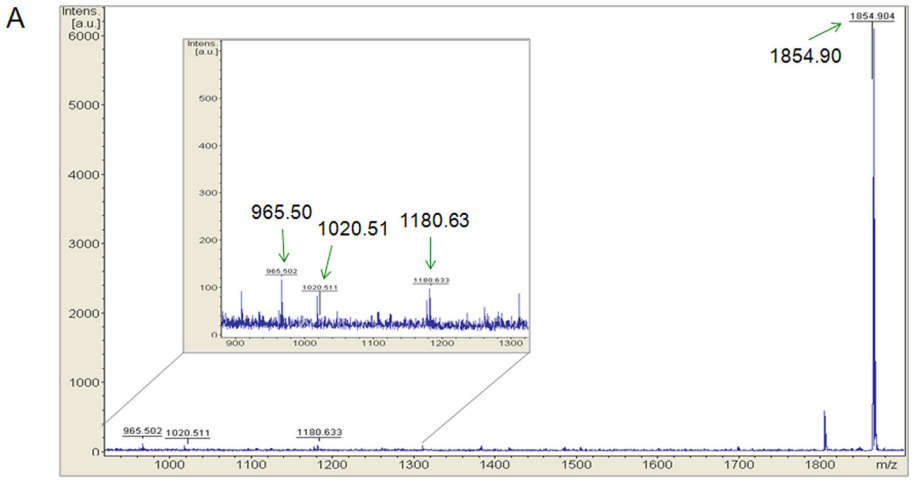

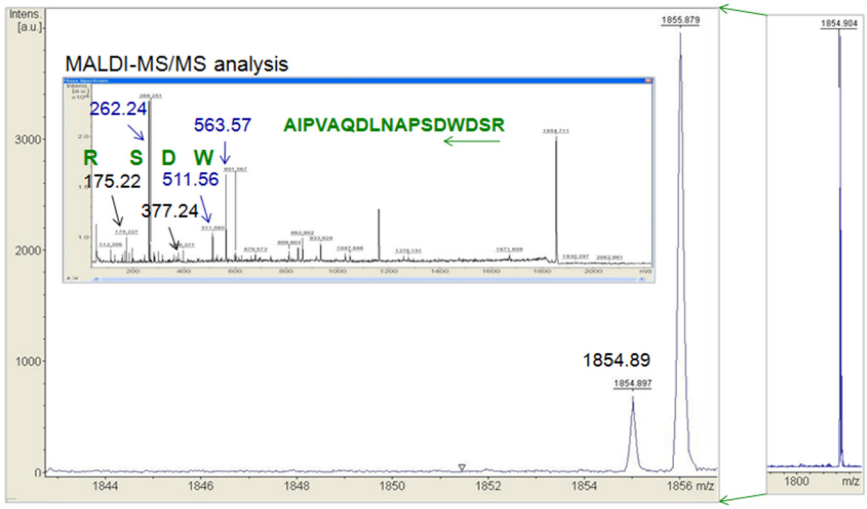

C

MS-Digest: Human Osteopontin Precursor
Trypsin Digest

Number	m/z (mi)	m/z (av)	Start	End	Sequence
1	802.4305	802.9080	71	77	(K)QETLPSK(S)
1	898.4629	898.9972	293	299	(K)EEDKHLK(F)
*1	965.5051	966.0882	160	168	(R)GDSVVYGLR(S)
*1	1020.4116	1020.9879	21	30	K)QADSGSSEEK(Q)
1	1037.4382	1038.0186	21	30	(K)QADSGSSEEK(Q)
*1	1180.6321	1181.3420	160	170	(R)GDSVVYGLRS K(S)
1	1387.6336	1388.4392	302	314	(R)ISHELDSASSEVN(-)
1	1666.7555	1667.7368	21	35	(K)QADSGSSEEKQLYNK(Y)
1	1683.7820	1684.7675	21	35	(K)QADSGSSEEKQLYNK(Y)
1	1690.8031	1691.8056	300	314	(K)FRISHELDSASSEVN(-)
1	1801.8755	1802.9935	36	51	(K)YPDAVATWLNPDPSQK(Q)
*1	1854.8981	1856.0141	204	220	(K)AIPVAQDLNAPSDWDSR(G)
1	1877.0461	1878.4705	3	20	(R)IAVICFCLLGITCAIPVK(Q)

Osteopontin Precursor (amino acid sequence):

1 MRIAVICFCLLGITCAIPVKQADSGSSEEKQLYNKYPDAVATWLNPDPSQKQNLLAPQNAVSSEETNDFKQETLPSKSNE
81 SHDHMDDMDDEDDDDHVDSQDSIDSNDSDDVDDTDDSHQSDESHHSDESDELVTDFPTDLPATEVFTPVVPTVDTYDGRG
161 DSVVYGLRSKSKKFRRPDIQYPDATDEDITSHMESEELNGAYKAIPVAQDLNAPSDWDSRGKDSYETSQLDDQSAETHSH
241 KQSRLYKRKANDESNEHSDVIDSQELSKVSREFHSHEFHSHEDMLVVDPKSKEEDKHLKFRISHELDSASSEVN

Protein Prospector search of the SwissProt.2008.06.10 database yielded a match to peptides of human osteocalcin precursor (Pre-OC) for protein peptides derived from the S4 spot (page 34 to 47 of supplemental Data). Notably, detection of Pre-OPN and Pre-OC can also be used as a predictor of the high quality of our protein extracts. Interestingly, mature OC serves as a

FIG. 4. ***A*, MALDI mass spectrum of a tryptic digest of a protein from the S1 spot (Fig. 3*A*).** The inset shows the enlarged region of the spectrum. The ion with *m/z* 965.50 corresponds to the peptide GDSVVYGLR (160–168 amino acids (AAs) of the Pre-OPN sequence), *m/z* 1020.41 to QADSGSSEEK (21–30 AAs), *m/z* 1180.63 to GDSVVYGLRSK (160–170 AAs) and *m/z* 1854.90 to AIPVAQDLNAPSDWDSR (204–220 AAs), respectively. The peptide sequences were further confirmed using MALDI-MS/MS analysis. *B*, Example of the MALDI-MS/MS analysis performed on the AIPVAQDLNAPSDWDSR peptide. The *m/z* 1854.90 peak is shown at a higher resolution. The MS/MS fragmentation scan was performed from *m/z* 100–2000 (supplemental Fig. S6). The collected spectrum, including the example of identifying first four amino acids (reversed order) based on a manual calculation of their *m/z*, is shown as the inset. Submission of the whole peptide fragment ion data to a MASCOT MS/MS ion search of the SwissProt database yielded a match to human osteopontin with the ions score –10*Log(P) and $p < 0.05$ (pages 48 to 53 of supplemental Data). *C*, the ProteinProspector MS-Digest performed *in silico* on the human OPN precursor using trypsin shows peptides and their corresponding *m/z* values (shown only up to 1878.5). The peptides present in the MALDI mass spectrum in Fig. 3*A* are marked with the stars. Location of the detected peptides on the amino acid sequence of the human OPN precursor is pictured below. The peptides from tryptic digest are marked in green. The two amino acid difference, in the length between two peptides (*m/z* 1020.41 and 1180.63) from the same Pre-OPN region, is shown in *red*. The peptide detected after chymotrypsin digest is shown in *blue*.

common marker of bone formation whereas OPN is known to be an inhibitor of mineralization. Thus, we wondered to what degree the level of these two proteins differs between the osteonal and interstitial tissue. Because using SDS-PAGE analysis generally provides only an approximation of quantitative protein differences, we used ELISA to quantify precisely the difference levels of OC and OPN in osteonal and interstitial tissues.

Higher OC and OPN Content in Osteonal than Interstitial Bone—ELISA allows rapid screening and quantitation of samples for the presence of antigen (here, OPN and OC) using specific antibodies. Notably, we used the OC ELISA assay that facilitated measurement of intact human OC. One bone piece was sufficient to collect accurate quantitative data from the OPN and OC ELISA experiments. There was 20 times or more OC present in osteonal bone (293×10^{-3} ng/μm^3 bone) than interstitial one. The level of OPN (16.13×10^{-3} ng/μm^3 bone) was also higher in the osteonal bone, but not as pronounced as compared with OC. The amounts of OPN and OC were lower in the interstitial bone (OC = 7.07×10^{-3} ng/μm^3 bone, OPN = 5.95×10^{-3}ng/μm^3 bone). Consequently, osteonal bone had higher OC and OPN contents than its spatially weight-matched interstitial bone. These data may be interpreted from the perspective of normal bone remodeling, which is based on a demonstrated ability of OC and OPN to alter bone remodeling (4–7, 53–60) or in terms of bone damage formation (47, 61–63) where the observed differences in the levels of these two proteins may act in conjunction with bone mineralization and glycation to influence microdamage formation and repair in bone.

Concluding Remarks—Bone proteomics is an emerging field. Our studies demonstrate that comprehensive biochemical analysis of bone matrix proteins using nanoscale amounts of bone tissue is feasible. The main methodological innovation is the development of the strategy combining laser-capture microdissection method of fully mineralized bone tissue with several new UPLC methods for determination of advanced glycation end products in proteins (here, collagen). Dissection of structural components of fully mineralized bone at the presented level of homogeneity has not been achieved before. Hierarchical separation of bone-matrix proteins using two-dimensional SDS-PAGE can serve as particularly useful tool to investigate changes and/or variation in the most abundant pools of bone proteins when a very limited amount of bone sample is available, or more broadly, for separation of similar amounts of proteins isolated from different biological materials displaying hierarchical protein abundance. In combination with MALDI TOF/TOF MS and MS/MS, this study opens a new avenue for bone research. However, our work is not only important for bone research alone but is of general significance to other fields including forensic, biology, anthropology and archaeology, where bone samples could truly be rare, small, and precious (19).

Application of the developed methods revealed that proteins, here collagen, from older tissues contain higher levels of AGEs and other crosslinks than the young tissue (43, 44, 50). Although our PYD/DPD data agree with those reported for whole bone (51, 52) and large osteonal and interstitial bone cores (34), PEN values in our studies show the opposite trend as compared with the published results. Specifically, in contrast to Nyman *et al.* (34), we found significantly higher PEN levels in older interstitial tissue than younger osteonal bone. We ascribe the observed differences to exceptional purity and uniformity of the dissected tissues using LCM. As age of osteons, and thus, their level of mineralization, collagen content and its degree of crosslinking normally tend to vary, it seems that our minute bone samples covered the areas of osteons of similar tissue age. Notably, our data agree with the mechanism and time-frame of PEN formation in long-lived tissues (32). In addition, our previous studies showed that accumulation of nonenzymatic glycation end-products in cortical bone causes stiffening of the type I collagen network and this may explain some of the age-related increase in skeletal fragility and fracture risk (33).

When investigating protein contents in osteonal *versus* interstitial bone tissue, we found that there was a greater prevalence of OPN and OC in osteonal bone, and this has not been shown before. These data may be interpreted in the context of normal bone remodeling or in terms of damage formation. Because both OPN and OC have been shown to regulate bone remodeling (4–7, 53–60) and microdamage formation (47, 61–63), the observed differences in their quantity may act in concert with bone mineralization and glycation (33) to influence microdamage and repair in bone.

Acknowledgments—We thank Dr. Evelyne Gineyts (University of Lyon, Lyon, France) for providing reagents for hydroxyproline determination by HPLC and Dr. Dmitri Zagorevski (Rensselaer Polytechnic Institute, Troy, NY) for technical assistance with the MALDI-TOF/TOF MS machine. G. E. S. thanks Dr. Mirco Sorci (Rensselaer Polytechnic Institute, Troy, NY) for stimulating discussions.

* This research was supported by National Institutes of Health (NIH) grants AG20618 and AR4963506-11 (D. V.). We acknowledge use of human bone tissues provided by the National Disease Research Interchange (NDRI) with support from NIH grant 5 U42 RR006042.

¶ To whom correspondence should be addressed: CIBIS 3137, Rensselaer Polytechnic Institute, 110 Eighth Street, Troy, NY 12180-3590, USA. Fax: 518-276-3035; E-mail: vashid@rpi.edu.

[S] This article contains supplemental Data along with Figs. S1 to S6 and Tables S1 and S2.

‖ Ethics/Animal Committee (IRB/ACUC) does not apply to this case (cadaveric human tissue).

Author Contributions: G. E. S. originated, developed and performed the experiments, analyzed the data, wrote the manuscript, designed and made the figures. L. K. assisted with bonding of bone sections to membrane slides for LCM. W. C. facilitated the two-dimensional SDS-PAGE work and critically reviewed the manuscript. D. V. originated and supervised the project, supplied resources and critically discussed and reviewed the manuscript.

REFERENCES

1. Balooch, G., Balooch, M., Nalla, R. K., Schilling, S., Filvaroff, E. H., Marshall, G. W., Marshall, S. J., Ritchie, R. O., Derynck, R., and Alliston, T.

(2005) TGF-β regulates the mechanical properties and composition of bone matrix. *Proc. Natl. Acad. Sci. U.S.A.* **102,** 18813–18818
2. Ducy, P., Desbois, C., Boyce, B., Pinero, G., Story, B., Dunstan, C., Smith, E., Bonadio, J., Goldstein, S., Gundberg, C., Bradley, A., and Karsenty, G. (1996) Increased bone formation in osteocalcin-deficient mice. *Nature* **382,** 448–452
3. Fantner, G. E., Adams, J., Turner, P., Thurner, P. J., Fisher, L. W., and Hansma, P. K. (2007) Nanoscale ion mediated networks in bone: osteopontin can repeatedly dissipate large amounts of energy. *NanoLetters* **7,** 2491–2498
4. Rittling, S. R., Matsumoto, H. N., McKee, M. D., Nanci, A., An, X. R., Novick, K. E., Kowalski, A. J., Noda, M., and Denhardt, D. T. (1998) Mice lacking osteopontin show normal development and bone structure but display altered osteoclast formation in vitro. *J. Bone Miner. Res.* **13,** 1101–1111
5. Razzouk, S., Brunn, J. C., Qin, C., Tye, C. E., Goldberg, H. A., and Butler, W. T. (2002) Osteopontin posttranslational modifications, possibly phosphorylation, are required for in vitro bone resorption but not osteoclast adhesion. *Bone* **30,** 40–47
6. Boskey, A. L., Spevak, L., Paschalis, E., Doty, S. B., and McKee, M. D. (2002) Mineral and matrix changes in bones of osteopontin-deficient mice. *Calcif. Tissue Int.* **71,** 145–154
7. Boskey, A. L., Spevak, L., Paschalis, E., Doty, S. B., and McKee, M. D. (2002) Osteopontin deficiency increases mineral content and mineral crystalinity in mouse bone. *Calcif. Tissue Int.* **71,** 145–154
8. Fisher, L. W., Hawkins, G. R., Tuross, N., and Termine, J. D. (1987) Purification and partial characterization of small proteoglycans I and II, bone sialoproteins I and II, and osteonectin from mineral compartment of developing human bone. *J. Biol. Chem.* **262,** 9702–9708
9. Hauschka, P. V., Lian, J. B., Cole, D. E., and Grundberg, C. M. (1989) Osteocalcin and matrix gla protein: vitamin K dependent proteins in bone. *Physiol. Rev.* **69,** 990–1034
10. Young, M. F. (2003) Bone matrix proteins: their function, regulation, and relationship to osteoporosis. *Osteoporosis Int.* **14 (Suppl 3),** S35–S42
11. Gundberg, C. M., Anderson, M., Dickson, I., and Gallop, P. M. (1986) "Glycated" osteocalcin in human and bovine bone. The effect of age. *J. Biol. Chem.* **261,** 14557–14561
12. Saito, M., Fujii, K., Soshi, S., and Tanaka, T. (2006) Reductions in degree of mineralization and enzymatic collagen cross-links and increases in glycation-induced pentosidine in the femoral neck cortex in cases of femoral neck fracture. *Osteoporos Int.* **17,** 986–995
13. Vashishth, D. (2007) The role of the collagen matrix in skeletal fragility. *Curr. Osteop. Rep.* **5,** 62–66
14. Tang, S. Y., Zeenath, U., and Vashishth, D. (2007) Effects of non-enzymatic glycation on cancellous bone fragility. *Bone* **40,** 1144–1151
15. Vashishth, D. (2004) Rising crack growth resistance behavior in cortical bone: Implications for toughness measurements. *J. Biomechanics* **37,** 943–946
16. Sornay-Rendu, E., Boutroy, S., Munoz, F., and Delmas, P. D. (2007) Alterations of cortical and trabecular architecture are associated with fractures in postmenopausal women, partially independent of decreased BMD measured by DXA: the OFELY study. *J. Bone Miner. Res.* **22,** 425–433
17. Vashishth, D. (2005) Collagen glycation and its role in fracture properties of bone. *J. Musculoskeletal Neuronal Interact.* **5,** 316
18. Schmidt-Schultz, T. H., and Schultz, M. (2004) Bone protects proteins over thousands of years: extraction, analysis, and interpretation of extracellular matrix proteins in archeological skeletal remains. *Am. J. Physical Anthropol.* **123,** 30–39
19. Nielsen-Marsh, C. M., Richards, M. P., Hauschka, P. V., Thomas-Oates, J. E., Trinkaus, E., Pettitt, P. B., Karavanic, I., Poinar, H., and Collins, M. J. (2005) Osteocalcin protein sequences of Neanderthals and modern primates. *Proc. Natl. Acad. Sci. U.S.A.* **102,** 4409–4413
20. Emmert-Buck, M. R., Bonner, R. F., Smith, P. D., Chuaqui, R. F., Zhuang, Z., Goldstein, S. R., Weiss, R. A., and Liotta, L. A. (1996) Laser capture microdissection. *Science* **274,** 998–1001
21. Espina, V., Wulfkuhle, J. D., Calvert, V. S., VanMeter, A., Zhou, W., Coukos, G., Geho, D. H., Petricoin, E. F., 3rd, and Liotta, L. A. (2006) Laser capture microdissection. *Nat. Protoc.* **1,** 586–603
22. Huffman, N. T., Keightley, J. A., Chaoying, C., Midura, R. J., Lovitch, D., Veno, P. A., Dallas, S. L., and Gorski, J. P. (2007) Association of specific proteolytic processing of bone sialoprotein and bone acidic glycoprotein-75 with mineralization within biomineralization foci. *J. Biol. Chem.* **282,** 26002–26013
23. Dahia, C. L., Mahoney, E. J., Durrani, A. A., and Wylie, C. (2009) Postnatal growth, differentiation, and aging of the mouse intervertebral disc. *Spine* **34,** 447–455
24. Hoffmann, M., Olson, K., Cavender, A., Pasqualini, R., Gaikwad, J., and D'Souza, R. N. (2001) Gene expression in a pure population of odontoblasts isolated by laser-capture microdissection. *J. Dent. Res.* **80,** 1963–1967
25. Young, C. S., Terada, S., Vacanti, J. P., Honda, M., Bartlett, J. D., and Yelick, P. C. (2002) Tissue engineering of complex tooth structures on biodegradable polymer scaffolds. *J. Dent. Res.* **81,** 695–700
26. Yao, S., Ring, S., Henk, W. G., and Wise, G. E. (2004) In vivo expression of RANKL in the rat dental follicle as determined by laser capture microdissection. *Archives of Oral Biology* **49,** 451–456
27. Shur, I., Socher, R., Hameiri, M., Fried, A., and Benayahu, D. (2006) Molecular and cellular characterization of SEL-OB/SVEP1 in osteogenic cells *in vivo* and *in vitro*. *J. Cell. Physiol.* **206,** 420–427
28. Swolin-Eide, D., Dahlgren, J. C., Nilsson, C., Albertsson-Wikland, K., Holmäng, A., and Ohlsson, C. (2002) Affected skeletal growth but normal bone mineralization in rat offspring after prenatal dexamethasone exposure. *J. Endocrinol.* **174,** 411–418
29. Roschger, P., Matsuo, K., Misof, B. M., Tesch, W., Jochum, W., Wagner, E. F., Fratzl, P., and Klaushofer, K. (2004) Normal mineralization and nanostructure of sclerotic bone in mice overexpressing Fra-1. *Bone* **34,** 776–782
30. Rodan, G. A., and Martin, T. J. (2000) Therapeutic approaches to bone diseases. *Science* **289,** 1508–1514
31. Rubin, C., Turner, A. S., Bain, S., Mallinckrodt, C., and McLeod, K. (2001) Anabolism: Low mechanical signals strengthen long bones. *Nature* **412,** 603–604
32. Saito, M., and Marumo, K. (2010) Collagen cross-links as a determinant of bone quality: a possible explanation for bone fragility in aging, osteoporosis, and diabetes mellitus. *Osteoporosis Int.* **21,** 195–214
33. Vashishth, D., Gibson, G. J., Khoury, J. I., Schaffler, M. B., Kimura, J., and Fyhrie, D. P. (2001) Influence of nonenzymatic glycation on biomechanical properties of cortical bone. *Bone* **28,** 195–201
34. Nyman, J. S., Roy, A., Acuna, R. L., Gayle, H. J., Reyes, M. J., Tyler, J. H., Dean, D. D., and Wang, X. (2006) Age-related effect on the concentration of collagen crosslinks in human osteonal and interstitial bone tissue. *Bone* **39,** 1210–1217
35. Seck, T., Scheppach, B., Scharla, S., Diel, I., Blum, W. F., Bismar, H., Schmid, G., Krempien, B., Ziegler, R., and Pfeilschifter, J. (1998) Concentration of insulin-like growth factor (IGF)-I and -II in iliac crest bone matrix from pre- and postmenopausal women: relationship to age, menopause, bone turnover, bone volume, and circulating IGFs. *J. Clin. Endocrinol. Metab.* **83,** 2331–2337
36. Dong, X. N., Yeni, Y. N., Zhang, B., Les, C. M., Gibson, G. J., and Fyhrie, D. P. (2005) Matrix concentration of insulin-like growth factor I (IGF-I) is negatively associated with biomechanical properties of human tibial cancellous bone within individual subjects. *Calcif. Tissue Int.* **77,** 37–44
37. Araya, S., Saito, S., Nakanishi, S., and Kawanishi, Y. (1961) Soluble collagen in bone. *Nature* **192,** 758–759
38. Mills, B. G., and Bavetta, L. A. (1966) Variations in extractable collagen of bone and skin with age and growth. *J. Gerontol.* **21,** 449–454
39. Bailey, A. J., and Peach, C. M. (1971) The chemistry of collagen crosslinks. *Biochem. J.* **121,** 257–259
40. Gharahdaghi, F., Weinberg, C. R., Meagher, D. A., Imai, B. S., and Mische, S. M. (1999) Mass spectrometric identification of proteins from silver-stained polyacrylamide gel. A method for the removal of silver ions to enhance sensitivity. *Electrophoresis* **20,** 601–605
41. Schmidt-Schultz, T. H., and Schultz, M. (2007) Well preserved non-collagenous extracellular matrix proteins in ancient human bone and teeth. *Int. J. Osteoarchaeol.* **17,** 91–99
42. Koch, K. R. (1988) *Parameter Estimation and Hypothesis Testing in Linear Models*, Springer-Verlag, Berlin
43. Allen, M. R., Gineyts, E., Leeming, D. J., Burr, D. B., and Delmas, P. D. (2008) Bisphosphonates alter trabecular bone collagen cross-linking and isomerization in beagle dog vertebra. *Osteoporosis Int.* **19,** 329–337
44. Saito, M., Marumo, K., Fujii, K., and Ishioka, N. (1997) Single-column high-performance liquid chromatographic-fluorescence detection of im-

mature, mature, and senescent crosslinks of collagen. *Anal. Biochem.* **253,** 26–32
45. Sroga, G. E., and Vashishth, D. (2011) UPLC methodology for identification and quantitation of naturally fluorescent crosslinks in proteins: a study of bone collagen. *J. Chromatogr. B*, **879,** 379–385
46. Price, P. A., Otsuka, A. A., Poser, J. W., Kristaponis, J., and Raman, N. (1976) Primary structure of the γ-carboxyglutamic acid-containing protein from bovine bone. *Proc. Natl. Acad. Sci. U.S.A.* **73,** 1447–1451
47. Poundarik, A., Karim, L., Gundberg, C., and Vashishth, D. The role of osteocalcin in bone fracture. *Proceedings of the 55th Meeting of the Orthopaedic Research Society* 2009, Las Vegas Feb. 22–25, 724
48. Ingram, R. T., Park, Y. K., Clarke, B. L., and Fitzpatrick, L. A. (1994) Age- and gender-related changes in the distribution of osteocalcin in the extracellular matrix of normal male and female bone: possible involvement of osteocalcin in bone remodeling. *J. Clin. Invest.* **93,** 989–997
49. Odetti, P., Rossi, S., Monacelli, F., Poggi, A., Cirnigliaro, M., Federici, M., and Federici, A. (2005) Advanced glycation end products and bone loss during aging. *Annals of the New York Academy of Sciences* **1043,** 710–717
50. Viguet-Carrin, S., Roux, J. P., Arlot, M. E., Merabet, Z., Leeming, D. J., Byrjalsen, I., Delmas, P. D., and Bouxsein, M. L. (2006) Contribution of the advanced glycation end product pentosidine and of maturation of type I collagen to compressive biomechanical properties of human lumbar vertebrae. *Bone* **39,** 1073–1079
51. Hernandez, C. J., Tang, S. Y., Baumbach, B. M., Hwu, P. B., Sakkee, A. N., van der Ham, F., DeGroot, J., Bank, R. A., and Keaveny, T. M. (2005) Trabecular microfracture and the influence of pyridinium and non-enzymatic glycation-mediated collagen cross-links. *Bone* **37,** 825–832
52. Valcourt, U., Merle, B., Gineyts, E., Viguet-Carrin, S., Delmas, P. D., and Garnero, P. (2007) Non-enzymatic glycation of bone collagen modifies osteoclastic activity and differentiation. *J. Biol. Chem.* **282,** 5691–5703
53. Eriksen, E. F. (1986) Normal and pathological remodeling of human trabecular bone: three dimensional reconstruction of the remodeling sequence in normals and in metabolic bone disease. *Endocr. Rev.* **7,** 379–408
54. Eriksen, E. F., Gundersen, H. J., Melsen, F., and Mosekilde, L. (1984) Reconstruction of the formative site in iliac trabecular bone in 20 normal individuals employing a kinetic model for matrix and mineral apposition. *Metab. Bone Dis. Relat. Res.* **5,** 243–252
55. Frost, H. M. (1965) A synchronous group of mammalian cells, whose *in vivo* behavior can be studied. *Henry Ford Hosp. Med. Bull.* **13,** 161–172
56. Jaworski, Z. F., Duck, B., and Sekaly, G. (1981) Kinetics of osteoclasts and their nuclei in evolving secondary Haversian systems. *J. Anat.* **133,** 397–405
57. Kimmel, D. B. (1980) A light microscopic description of osteoprogenitor cells or remodeling bone in the adult. *Metab. Bone Dis. Relat. Res.* **2 (Suppl.),** 181
58. McKee, M. D., and Nanci, A. (1996) Osteopontin: an interfacial extracellular matrix protein in mineralized tissues. *Connect. Tissue Res.* **35,** 197–205
59. Boskey, A. L., Gadaleta, S., Gundberg, C., Doty, S. B., Ducy, P., and Karsenty, G. (1998) Fourier transform infrared microspectroscopic analysis of bones of osteocalcin-deficient mice provides insight into the function of osteocalcin. *Bone* **23,** 187–196
60. Kazanecki, C. C., Uzwiak, D. J., and Denhardt, D. T. (2007) Control of osteopontin signaling and function by post-translational phosphorylation and protein folding. *J. Cell. Biochem.* **102,** 912–924
61. Diab, T., Condon, K. W., Burr, D. B., and Vashishth, D. (2006) Age-related change in the damage morphology of human cortical bone and its role in bone fragility. Bone **38,** 427–431
62. Diab, T., and Vashishth, D. (2007) Morphology, localization and accumulation of *in vivo* microdamage in human cortical bone. *Bone* **40,** 612–618
63. Sroga, G. E., Karim, L., and Vashishth, D. Increased levels of osteocalcin and osteopontin correlate with bone microdamage. *Proceedings of the 55th Meeting of the Orthopaedic Research Society* 2009, Las Vegas Feb 22–25, 2990